EntoScan and BEEomass: a standardized imaging system and a physically motivated model for high-throughput dry biomass estimation of arthropods

Melika Baghooee [1,*], Robert Thalheim [2], Fevziye Hasan [3], Søren Toft [4], Torsten Nygård Kristensen [1,5], and Quentin Geissmann [1]

[1]Center for Quantitative Genetics and Genomics, Aarhus University, Denmark

[2]City University of Applied Sciences Bremen, Germany

[3]Museum of Evolution, Uppsala University, Sweden

[4]Department of Biology, Aarhus University, Denmark

[5]Department of Chemistry and Bioscience, Aalborg University, Denmark

[*]Corresponding author: melika@qgg.au.dk

Abstract

Computer vision and AI are now widely used for automated insect classification, but their potential for estimating other traits, such as biomass, is not yet fully explored. Insect biomass is a key measure of ecosystem function, informing ecosystem services, food webs, and environmental change. It is also used to track population trends and estimate the contribution of insects to ecosystem carbon. Currently, wet bulk biomass is used as a standard measure for insect monitoring because it is fast and practical. However, bulk biomass conflates individual contributions, obscuring biologically meaningful variation. Obtaining individual-level biomass is challenging as each specimen must be dried and weighed, making large-scale measurements practically intractable. Here, we propose EntoScan, an open-source, low-cost and standardized imaging system based on a modified flatbed scanner and Biomass Estimation in Entomology (BEEomass), a novel computer vision model that estimates dry biomass of terrestrial arthropods from images alone. BEEomass uses a physically motivated, scale-invariant representation of body size and mass that allows it to generalize across taxa differing widely in morphology. We show that this image-based approach provides accurate dry biomass estimates (R^2 >0.95) while considerably reducing both the manual effort and specimen destruction compared to direct weighing. We then illustrate the practical utility of EntoScan and BEEomass through two proof-of-concept case studies: tracking temperature-induced size variation in laboratory-reared *Drosophila* and monitoring seasonal biomass dynamics in wild-caught *Pachygnatha degeeri*. Because they are affordable, scalable, and easy to use, our two methods have the potential to serve as standardized tools for monitoring insect biomass at scale, and ultimately improve our ability to quantify and predict ecosystem functions and services, supporting more effective

conservation and agricultural management.

1 Introduction

The collection and identification of large numbers of insects is becoming more automated, for example through the use of image-based classification systems, automated traps, and machine learning approaches (Ferro and Summerlin [2019], Karlsson et al. [2020], Geissmann et al. [2022], Gharaee et al. [2024], Sittinger et al. [2024]). But quantifying other variables at scale, such as traits, remains challenging, as obtaining measurements from individual specimens still relies on manual, time-consuming methods. One such trait is biomass, which is often used to provide insights into ecosystem processes. For example, it has been used to study pollination (Kendall et al. [2019],Vereecken et al. [2021]), decomposition, food web interactions (Yang and Gratton [2014]), and changes over time and across environmental gradients (Hallmann et al. [2017], Uhler et al. [2021]).

Obtaining biomass measurements for individual insects is difficult due to their small size and fragile nature. While bulk measurements allow large numbers of samples to be processed efficiently (Hallmann et al. [2017]), many ecological, evolutionary, and applied questions require trait information at the level of the individual organism, including variation within and between species and across environmental gradients (Karan et al. [1998]), Lister and Garcia [2018]). However, measuring biomass at the level of individual organisms typically requires drying and weighing each specimen, which is time-consuming and limits scalability. This provides an opportunity to develop automated methods to estimate individual biomass and other morphological traits while improving throughput. Recent studies have started to explore the potential of estimating biomass from images of individual organisms. For example, Impiö et al. [2026] estimate biomass by fitting linear models using area and sinking speed of specimens in liquid as predictors, Shirali et al. [2025] estimate morphological traits such as length or area that can be used as proxies for biomass, Schneider et al. [2022] estimate biomass from images of bulk samples using calibration samples with known weights and corresponding pixel counts, and Ärje et al. [2020] estimate biomass by fitting statistical models relating specimen area to measured dry weight. These approaches vary in their strategies, the taxa they target, and the imaging platforms they rely on, which differ in accessibility and reproducibility across laboratories. Together, these differences point to the need for a generalized and reproducible approach to biomass estimation.

Standardized image acquisition, combined with computer vision methods, has been widely used for insect classification (Geissmann et al. [2022], Wührl et al. [2023] Gharaee et al. [2024], Sittinger et al. [2024]). At the same time, images contain information on morphological traits such as size, which can be related to biomass (Shirali et al. [2025]), and incorporating such information into classification models has been shown to improve classification performance (Baghooee and

Geissmann [2026c]). This suggests that image-based methods could be used not only for classification but also for estimating quantitative traits.

Different imaging strategies have been used for insect samples. Systems designed for individual specimens can produce high-quality images under controlled conditions, as demonstrated by systems such as Biodiscover (Ärje et al. [2020]) and Entomoscope (Wührl et al. [2023]). However, these systems are often complex and may be difficult to implement in standard laboratory workflows. In contrast, bulk imaging approaches allow many specimens to be processed at once (Schneider et al. [2022]), but they may require considerable manual effort, which can limit their scalability.

Flatbed scanners provide an alternative that combines relatively low cost with consistent image quality. They produce high-resolution images with controlled lighting and fixed scale, which supports the standardization of color and size measurements (Schubert [2000], Mendez et al. [2018], Borlinghaus et al. [2024], Keasar et al. [2024], Schädel and Schubert [2024] Ong et al. [2025], Mavrianos et al. [2026]). Such systems have been successfully applied in contexts like herbarium digitization (Kovtonyuk et al. [2019]); however, standard scanners are not specifically designed for biological applications. Limitations include challenges related to focus, as specimens placed in containers above the scanner surface can fall outside the focal plane and appear out of focus, interfaces that are not adapted to experimental workflows, and limited flexibility for assigning metadata or organizing data in structured formats.

Here we present two related original contributions: (a) EntoScan, a standardized imaging system based on a modified flatbed scanner. The system is designed to be simple to use and compatible with typical laboratory workflows, and is provided as an open-source, well-documented solution to facilitate adoption by the broader research community (https://github.com/darsa-group/EntoScan). (b) Biomass Estimation in Entomology (BEEomass), a computer vision model for estimating dry biomass of arthropods from images (https://github.com/darsa-group/BEEomass). By combining the EntoScan with BEEomass, we show that, in addition to taking high-quality images, individual insect biomass can be reliably estimated directly from images using a novel formulation for biomass estimation. This approach enables the analysis of size and biomass across large numbers of specimens, supporting the study of variation within species and across environmental conditions. More broadly, it provides a scalable and practical alternative to traditional biomass measurements, extending the use of image-based methods beyond classification to the estimation of quantitative traits of biological importance, including fitness components. In addition, we provide an openly available dataset of paired images and dry biomass measurements, supporting further development of image-based biomass estimation methods (https://zenodo.org/records/20543262).

2 Methods

2.1 EntoScan

EntoScan is an open-source hardware-software platform designed for high-throughput imaging of arthropods, available at https://github.com/darsa-group/EntoScan. The system combines a modified flatbed scanner (Fig. 1a) with custom acquisition software and structured data storage (Fig. 1b; see also S1 for an operation video of the setup). The scanner provides a controlled imaging environment with uniform illumination and fixed geometry, which enables the reproducible acquisition of large numbers of specimens and ensures that specimen size and scale remain consistent across acquisitions. Our software allows the user to define acquisition regions, control resolution, and associate images with metadata through barcode-based identification, with all outputs stored in a structured format for downstream analysis.

2.1.1 Hardware

An Epson Perfection V850 Pro flatbed scanner (CCD-based) was selected and modified in this study (Fig. 1a). When imaged within containers, specimens are positioned above the focal plane of the scanner, resulting in reduced focus and image sharpness. To address this, the original glass platen was removed and replaced with a custom aluminum plate (250 × 378 × 3 mm) containing a central cut-out (178 × 230 mm) for holding a thinner (1 mm) glass. This design lowers the position of the container relative to the scanner optics and places the specimens closer to the focal plane. The aluminum plate was fixed in place using double-sided adhesive, and a white calibration strip was attached to its upper edge to preserve the scanner's exposure reference. To minimize movement during scanning, particularly when specimens were imaged in liquid, the scanner was placed on a concrete block with foam support to reduce vibrations and prevent color distortion in the images. A comparison between images acquired before and after modification is shown in Fig. 1c. This shows the modified setup improves image quality, with features such as tarsal claws, hairs, and legs appearing more clearly and sharply (see arrows). Further details of the scanner modification are available in the mentioned GitHub repository documentation. A step-by-step description of the modification is provided in the online documentation (https://github.com/darsa-group/EntoScan).

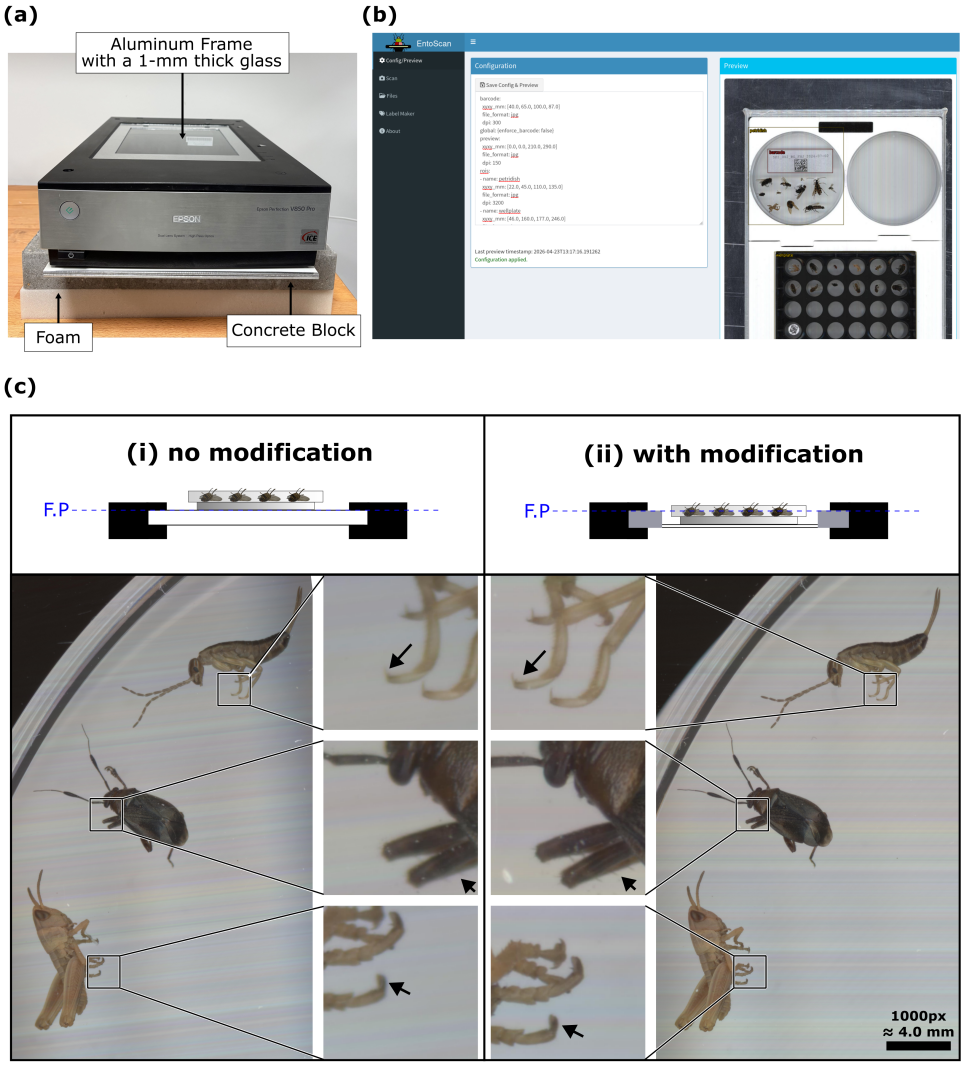

Figure 1: **(a) Hardware:** The scanner after modification (EntoScan). It is mounted on a stable base to minimize vibrations during scanning. **(b) Software:** Overview of the EntoScan software interface, showing the configuration of scan parameters and a preview of acquisition regions. **(c) Comparison of the resulting image quality before (i) and after (ii) modification**: Lowering the specimen plane improves focus, resulting in sharper images and increased visibility of fine morphological details (e.g., tarsal claws, hairs, and legs; see arrows). The shown regions represent only a small fraction of the full scan area

2.1.2 Software

Commercial scanner software is designed for general-purpose imaging and provides limited control over acquisition workflows. To use a scanner for biological studies, imaging requires the ability to define multiple regions within a single scan, control acquisition resolution, and associate images with external metadata. To support these requirements, we developed custom software as part of this study to control image acquisition and data handling (Fig. 1b), all orchestrated through a user-centric visual interface.

The scanner control service was implemented using a FastAPI backend, and it manages communication with the scanner hardware, executes scan commands, and generates previews of the acquisition layout. The user interface was developed in R Shiny, allowing users to configure scan

parameters through a structured configuration file, including the definition of regions of interest, acquisition resolution, and file format. The software is packaged as a Docker-based application, making it straightforward to install and deploy across systems. It also includes a database for storing and organizing image metadata. Additionally, a preview mode enables visualization of the scan layout prior to the acquisition. A demonstration of the imaging workflow, including sample preparation and software interaction, is provided in S1.

2.1.3 Data management

A custom two-dimensional barcode system was developed to provide unique specimen identifiers and enable linkage with associated metadata. Barcode labels were generated using a lightweight, open-source web application developed as part of this study (https://darsa.info/EntoScan-labels/) although any software capable of producing equivalent barcode formats can be used within the workflow. These barcodes are scanned together with the samples to associate each sample with its corresponding metadata. Each scan generates image files, thumbnails for rapid visualization, and a corresponding metadata file containing barcode-derived metadata, acquisition parameters, device information, and a checksum for data integrity. The data are organized hierarchically by acquisition time, scanner ID, and region of interest to ensure consistent naming and avoid conflicts across datasets, while all metadata are stored in a local database to allow rapid indexing and retrieval of images.

2.2 Dataset Collection

2.2.1 Arthropod samples

Specimens were collected using standard entomological bulk sampling methods, including pan traps in Denmark (Knudshoved Odde; June-July 2024), and Malaise traps in Sweden (Uppsala; April, June, and August 2025). Pan traps are colored bowl traps that attract mainly pollinators (e.g., Diptera). Malaise traps are tent-like net structures that guide flying insects into a collecting container and are efficient for semi-aquatic insects (Plecoptera, Ephemeroptera, and Trichoptera) and non-lepidopteran pollinators (Hymenoptera, Diptera, and Coleoptera) (Montgomery et al. [2021]). To include ground-dwelling arthropods, additional specimens, including beetles and spiders collected using a vacuum sampling method in Denmark, were also included in the dataset. In addition to these field-collected specimens, a subset of laboratory-reared *Drosophila* specimens was included in the dataset. The species were: *D. equinoxialis*, *D. lutescens*, *D. melanogaster*, *D. simulans*, and *D. virilis*

2.2.2 Image acquisition

To generate a dataset for investigating the potential of using a computer vision-based approach for estimating dry biomass of arthropods, specimens were imaged in 24-well plates. Each plate was assigned a unique identifier, and each specimen was labeled based on its plate ID and well position, ensuring that each specimen had a unique identifier. In all plates, well D6 was reserved for a two-dimensional barcode encoding the plate ID, which was used as metadata for the scan.

To account for variation in specimen pose, each plate was scanned four times. Between successive scans, specimens were manually repositioned within their wells, resulting in multiple images of the same individual under different orientations.

2.2.3 Biomass measurement

Following imaging, specimens were transferred to custom 3D-printed racks matching the layout of the well plates. These racks facilitated the transfer of specimens to the drying process while preserving their positional identity. Specimens were dried in an oven for 24 hours at 80°C to obtain dry biomass.

After drying, specimens were weighed individually using analytical balances with a minimum readability of 0.001 mg. Specimens imaged in Denmark were weighed using a Sartorius Quintix analytical balance, while specimens processed in Sweden were weighed using a Mettler Toledo AT261 DeltaRange analytical balance. In total, the dataset consists of approximately 8,400 images of 2,100 individual specimens paired with their corresponding dry biomass. The dataset is publicly available at https://zenodo.org/records/20543262.

2.3 BEEomass: the biomass estimation model

2.3.1 Dataset and image preprocessing

To evaluate the generalizability of the biomass estimation method on independently acquired data, we used 2037 images from the Biodiscover dataset (Ärje et al. [2020], Impiö et al. [2026]). The Biodiscover dataset consists of individually imaged arthropod specimens with corresponding dry biomass measurements, acquired using the Biodiscover system (Ärje et al. [2020]), a dual-camera imaging platform that captures specimens from two angles while they sink through an ethanol-filled cuvette.

Both datasets consist of multiple images per specimen. To prevent data leakage arising from these repeated observations, the data were split at the level of individual specimens, ensuring that all images of a given specimen were assigned to a single subset. The datasets were divided into 80% training, 10% validation, and 10% test sets using a random split stratified by specimen identity.

Before model training, individual specimens were segmented from the background using FlatBug

(Svenning et al. [2026]). The segmented images were resized such that the longest side was 224 pixels while preserving aspect ratio and padded with a white background to obtain square 224×224 images.

2.3.2 Area-based regression model

As a baseline, we implemented an area-based regression model to estimate biomass from the area of the segmented specimen. To reflect the expected scaling between body size and mass, we used the square root of the segmented area as a proxy for length and the cubic root of dry biomass as the response variable (Kühsel et al. [2017]). A linear model was fitted on the training data and then applied to the test set to generate predictions.

2.3.3 Biomass factor-based convolutional neural network (CNN) model

We aimed to predict insect dry biomass from images while minimizing dependence on absolute size. Each segmented image of an individual specimen i is associated with a measured dry biomass M_i (in mg), image dimensions (w_i, h_i) in pixels, and an acquisition resolution DPI_i (dots per inch).

Each segmented image is resized by a factor s_i such that its longest side equals 224 pixels, and then padded with a white background to obtain a square 224×224 RGB input while preserving the original aspect ratio. Given this resize factor, the physical width of the imaged field of view can be expressed as

$$L_i = 25.4 \frac{224/s_i}{\mathrm{DPI}_i}, \tag{1}$$

where L_i is expressed in millimeters and 25.4 is the conversion factor from inches to millimeters.

Rather than predicting biomass directly, we define a size-normalized "Biomass Factor (BF)"

$$\mathrm{BF}_i = \frac{M_i^{1/3}}{L_i}, \tag{2}$$

which has units of $\mathrm{mg}^{1/3}\,\mathrm{mm}^{-1}$. This quantity can be interpreted as a density-like measure capturing deviations from isometric scaling between mass and length (Fig. 2a). The relationship between specimens' length and biomass is shown in Fig. 2b for both datasets, where the cubic root of biomass increases approximately linearly with length. The distribution of biomass factor values for both datasets is shown in Fig. 2c, illustrating the range of values observed across specimens.

Under isometric scaling ($M \propto L^3$), BF is constant: doubling ($\times 2^1$) an organism's characteristic length results in an eightfold ($\times 2^3$)increase in mass (Kühsel et al. [2017]). Consequently, variation in BF reflects differences in mass relative to size, capturing morphological "compactness". In Fig. 2d, we show representative images associated with low and high BF values, illustrating how elongated insects (e.g. Culicidae) exhibit lower BF than more compact insects (e.g. Coleoptera) of comparable size.

At inference time, given a predicted biomass factor $\widehat{\mathrm{BF}}_i$ and the corresponding physical scale L_i, dry biomass is estimated as

$$\widehat{M}_i = \left(\widehat{\mathrm{BF}}_i \cdot L_i\right)^3. \tag{3}$$

2.3.4 Model training

Model architecture We used an EfficientNetV2 (Tan and Le [2019]) backbone (variant v2_s) initialised with ImageNet pertaining. The final layer was adapted for scalar regression, producing a single output BF per image.

Loss function The model was trained to minimise the mean squared error (MSE) between predicted and target biomass factors:

$$\mathcal{L}_{\mathrm{MSE}} = \frac{1}{N}\sum_{i=1}^{N}\left(\widehat{BF}_i - BF_i\right)^2 \tag{4}$$

Data augmentation and label smoothing During training only (not validation or test), we applied random augmentations of two kinds "scale augmentation" and "image augmentation".

Scale augmentation To simulate the same insect being imaged at a smaller physical scale. For each training sample, a scale factor was drawn as

$$s \sim \mathcal{U}(s_{\min}, 1), \quad s_{\min} = 0.5. \tag{5}$$

The entire 224×224 image was resized by a factor s and pasted, centred, onto a white 224×224 canvas. Because inferred mass scales cubically with linear size, the regression target was adjusted accordingly:

$$\mathrm{BF}' = \mathrm{BF} \cdot s^3. \tag{6}$$

This ensures that the learning task remains physically consistent under the synthetic change of scale.

Image augmentation In addition to the scale-consistent augmentation described above (training only), we applied the following photometric and geometric augmentations to improve robustness:

- Random horizontal flip ($p = 0.5$),
- Random rotation by multiples of 90° (uniformly sampled from $\{0, 90, 180, 270\}$), padding exposed regions with white,
- Colour jitter applied to brightness, contrast, saturation, and hue,
- Random choice between Gaussian blur (kernel size 3 or 9, $\sigma \in [0.1, 4.0]$) and sharpness adjustment (factor $\in [0.5, 2.0]$).

Label smoothing To mitigate overfitting to specific target values and to reflect uncertainty in measured biomass, we applied a per-sample multiplicative target jitter during training, used only for loss computation. For each sample, a multiplier was drawn as

$$m \sim \mathcal{U}(m_{\min}, m_{\max}), \quad m_{\min} = 0.8,\ m_{\max} = 1.2, \tag{7}$$

2.3.5 Optimisation and learning rate schedule

For training we used the AdamW optimiser with a learning rate of 1×10^{-4} and a weight decay of 1×10^{-5}. The model was trained for 500 epochs using mini-batches of 32 samples. The learning rate was reduced using a StepLR schedule every 100 epochs by a factor of 0.5.

2.3.6 Validation and model selection

The best-performing model was selected as the checkpoint achieving the lowest validation loss (mean squared error) on the validation set. The selected model was subsequently evaluated on the held-out test set.

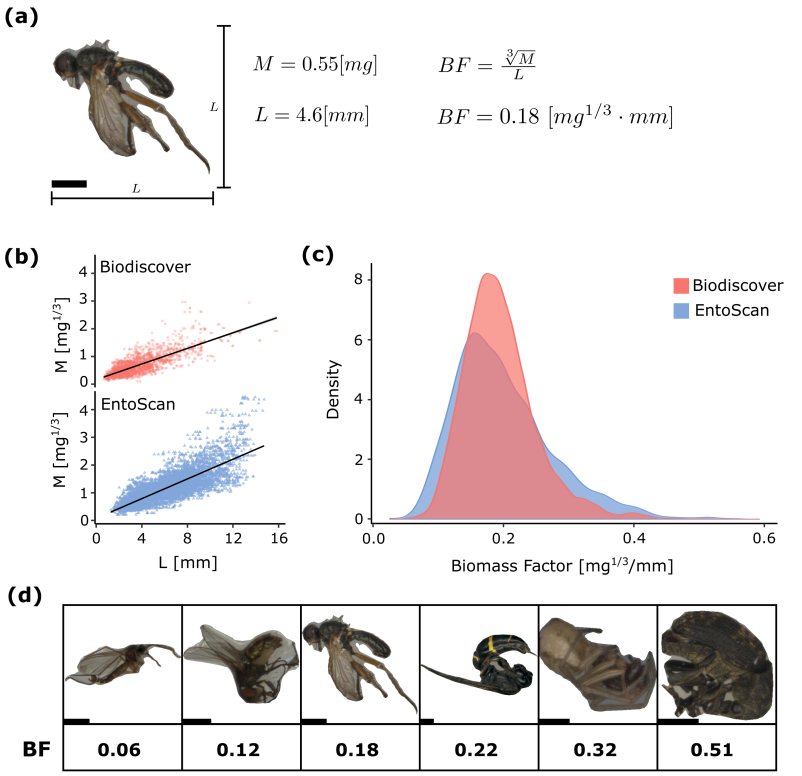

Figure 2: **Biomass factor definition.** (a) Illustration of the biomass factor (BF) calculation from dry mass M and body length L. (b) Linear relationship between the cubic root of dry mass M and body length L for the two datasets. (c) Distribution of biomass factor values for the two datasets. (d) Representative specimens spanning a range of BF values, showing the variation in body shape from elongated to compact morphologies. All scale bars represent 1 mm.

2.3.7 Implementation

Training the CNN model was implemented in PyTorch (Paszke et al. [2019]) and performed with GPU acceleration when available. All statistical analyses, including the area-based regression model, bootstrap-based performance evaluation, and ANOVA, were implemented in R (version 4.5.2) (R Core Team [2025]). Visualizations were generated using the ggplot2 package (Wickham [2016]). The code for training the model is available on our GitHub repository at https://github.com/darsa-group/BEEomass

2.3.8 Model evaluation

Model performance was evaluated on the test set using mean absolute error (MAE) and coefficient of determination (R^2). Because multiple images were available for each specimen, we used a bootstrap approach (500 iterations) to account for variability. In each iteration, one image per specimen was selected and resampled with replacement. Performance metrics were calculated for each iteration, and 95% confidence intervals were obtained from the resulting distributions.

This evaluation process was applied consistently to both the area-based linear regression model and the biomass factor-based CNN model.

2.4 Proof of concept

To evaluate whether the model can capture biologically meaningful variation in different contexts, we applied it to both controlled laboratory data and field-collected ecological samples.

2.4.1 Estimating biomass of *Drosophila* populations

Five *Drosophila* species were included in this study: *D. equinoxialis*, *D. lutescens*, *D. melanogaster*, *D. simulans*, and *D. virilis*. All species have been keept at 19°C at Aalborg University since 2018. The populations originate from different labs and stock centers (MacLean et al. [2019]). For normal maintenance, flies were kept at census population sizes of ca. 5000 individuals per generation. They were maintained at 20°C and 50% RH at a 12:12 h light/dark cycle and feed a standard Drosphila medium composed of dry yeast (60 g L^{-1}), sucrose (40 g L^{-1}), oatmeal (30 g L^{-1}), agar (16 g L^{-1}), Nipagin (12 mL L^{-1}) (Nipagin, Sigma-Aldrich, St. Louis, MO, USA), and acetic acid (1.2 mL L^{-1}). The flies used in this study were density controlled during development. This was done by collecting 50 eggs into 10 vials with 7 mL medium per species. Flies producing the eggs were between 5 and 10 days old. After collecting the eggs, 5 vials per species were exposed to 19°C, and 5 were exposed to 28°C. They were kept at these temperatures until they emerged as adults. Within 24 hours after emerging, flies from all species and temperatures were sexed and thereafter frozen in empty Eppendorf tubes. Thereafter, flies were imaged using the EntoScan workflow. The resulting images were used as input to the biomass estimation model to obtain predicted dry biomass values, which

were then compared across species, sex, and temperature conditions. See Supplementary Table 1 for the number of individuals scanned per species and temperature treatment.

Differences in biomass across species, sex, and temperature were assessed using analysis of variance (ANOVA). A linear model including all interaction terms was fitted, and a Type III ANOVA was performed. Analyses were conducted on log-transformed biomass values to better meet the assumptions of normality. Post-hoc pairwise comparisons were conducted using estimated marginal means (emmeans) to evaluate differences between temperature conditions within each species and sex.

2.4.2 Estimating biomass of ecological samples of the spider *Pachygnatha degeeri*

To assess performance on ecological samples, the model was applied to field-collected specimens of *Pachygnatha degeeri*. Specimens were collected between March 2023 and May 2025 from four sites in Central Jutland, Denmark (Fem Høje, Hørhaven, Moesgaard Strand, and Uth). The same imaging and analysis workflow as described for the *Drosophila* case study was applied to obtain predicted biomass distributions. In total, 1,913 individuals were imaged for this experiment within approximately 2.5 hours using EntoScan.

3 Results

3.1 Biomass Estimation Model

To assess whether the proposed biomass factor (BF)-based CNN model improves biomass estimation, we compared it to a standard area-based linear regression model (Fig. 3a). Predictions from the linear model showed greater dispersion, whereas the CNN predictions were more tightly clustered around the regression line. This improvement was consistent across both datasets. For the EntoScan dataset, the CNN achieved a significantly higher R^2 (0.95 [0.93, 0.97] vs. 0.75 [0.68, 0.81]) and lower MAE (0.08 [0.06, 0.09] vs. 0.20 [0.17, 0.23]) than the linear regression model. A similar improvement was observed for the Biodiscover dataset, where the CNN significantly increased R^2 (0.89 [0.81, 0.94] vs. 0.70 [0.59, 0.80]) and reduced the prediction error (MAE 0.07 [0.05, 0.10] vs. 0.14 [0.12, 0.17]), showing improved performance across datasets with differing characteristics.

3.2 Case I: *Drosophila*

Having established that the BF-based CNN model provides accurate biomass estimations, we next asked whether it captures biologically meaningful variation. To test this, we designed a controlled experiment based on a well-established pattern in the literature, where the body size of *Drosophila* is known to vary with developmental temperature (Karan et al. [1998]). After growing five *Drosophila* species at two different temperatures (19°C and 28°C) and imaging them with EntoScan, we used

the resulting images as input to the BF-based CNN model to estimate biomass (Fig. 3b).

Changes in temperature significantly reduced body size in four out of five species, in both males and females (Fig. 3b). This indicates that the method captures temperature-dependent variation in body size. An exception was observed for *D. virilis*, where no significant temperature effect was apparent. Sex also contributed to variation in predicted dry mass, with females generally being larger than males. These patterns are reflected in the significance annotations in Fig. 3b, and representative images (Fig. 3b) show corresponding differences in body size, with larger individuals observed at lower temperatures.

Together, these results show that the method provides robust and biologically relevant estimates of body size across species, sexes, and experimental conditions, while requiring substantially less effort than drying and weighing each specimen individually (2,070 individuals scanned in approximately 4.5 hours).

3.3 Case II: *Pachygnatha degeeri*

Finally, to evaluate the method under natural conditions, we applied it to field-collected spider specimens (Fig. 3c). Predicted dry mass varied across the sampling period, revealing temporal structure in body size distributions.

The species breeds in spring, with juvenile instars developing throughout the summer and reaching adulthood in early autumn. The heatmap shows two peaks in abundance: the first (day 170) corresponds to the emergence of juveniles following hatching from egg sacs, when population size is at its maximum, while the second (day 250) reflects the period when individuals have reached adulthood later in the season. These individuals do not reproduce in autumn but overwinter and breed the following spring, resulting in a lower population size during the reproductive period. This pattern is consistent with a univoltine life cycle and is supported by a previous study (Alderweireldt and De Keer [1990]).

Sexual size dimorphism, egg development in females, and the presence of both juvenile and adult individuals could contribute to the observed size distributions. Many arthropods undergo substantial changes in body size during development, and these patterns may also reflect differences in life stages within the sampled populations.

Overall, this result indicates that the method captures temporal variation in biomass across species collected from four different field sites and can support the study of seasonal dynamics in arthropod communities.

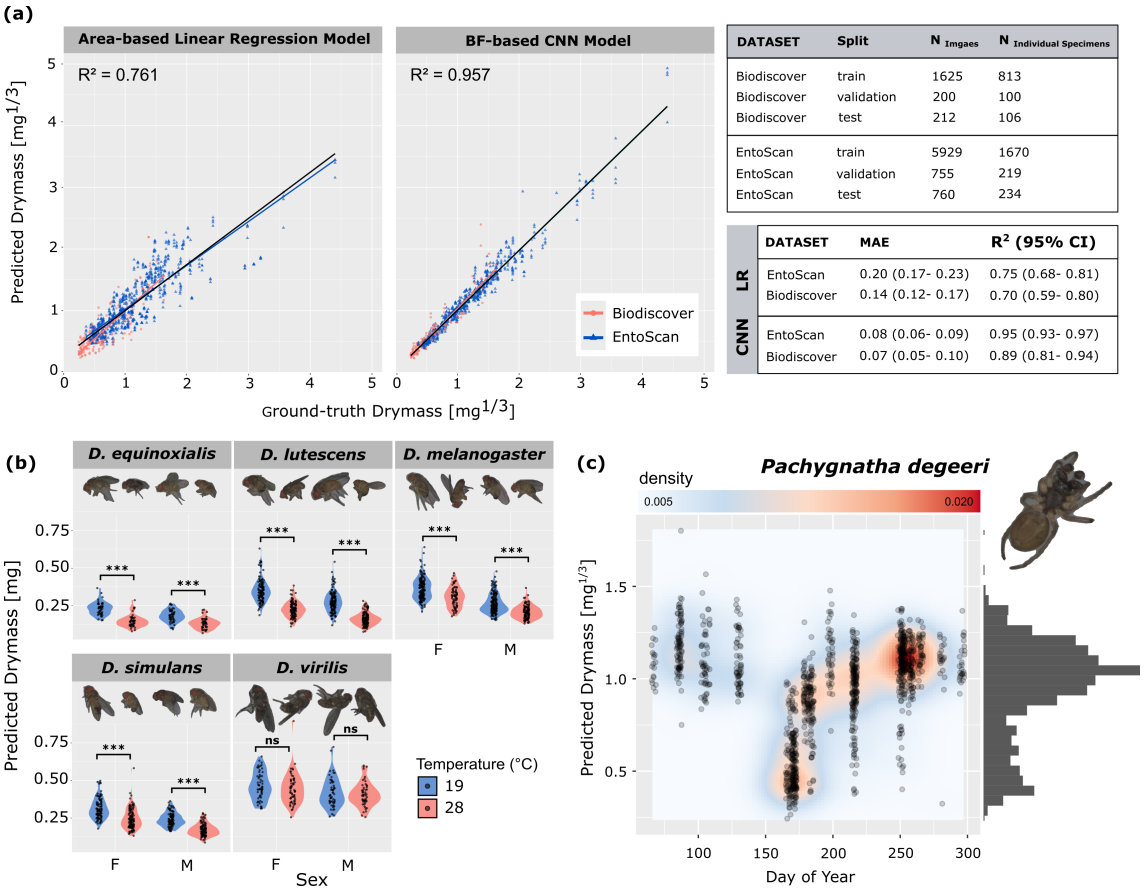

DATASET	Split	N Imgaes	N Individual Specimens
Biodiscover	train	1625	813
Biodiscover	validation	200	100
Biodiscover	test	212	106
EntoScan	train	5929	1670
EntoScan	validation	755	219
EntoScan	test	760	234

	DATASET	MAE	R^2 (95% CI)
LR	EntoScan	0.20 (0.17- 0.23)	0.75 (0.68- 0.81)
	Biodiscover	0.14 (0.12- 0.17)	0.70 (0.59- 0.80)
CNN	EntoScan	0.08 (0.06- 0.09)	0.95 (0.93- 0.97)
	Biodiscover	0.07 (0.05- 0.10)	0.89 (0.81- 0.94)

Figure 3: **Evaluation and application of the biomass estimation method across datasets and biological contexts**. (a) Comparison between an area-based linear regression model and the biomass factor (BF)-based CNN model using the Biodiscover and EntoScan datasets. Predicted dry mass is plotted against ground-truth measurements. The BF-based CNN model shows reduced dispersion and improved agreement across the full range of values. The table at the top reports the dataset composition, including the number of images and individuals in each data split. The table below reports model performance, showing mean absolute error (MAE) and coefficient of determination (R^2) for each model and dataset. (b) Predicted dry mass distributions for five *Drosophila* species, separated by sex and growth temperature (19°C and 28°C), together with representative images illustrating morphological and body size differences across sexes and temperatures. Across species, individuals grown at lower temperature have higher predicted dry mass, with significance indicated by asterisks (***, $p < 0.001$; ns, not significant), based on post-hoc pairwise comparisons using estimated marginal means. pecies, sex, and temperature treatments. (c) Temporal variation in predicted dry mass for the spider species *Pachygnatha degeeri*. 2D density plot from dry mass shows changes in body size over the sampling period, with species-specific patterns in seasonal variation.

4 Discussion

Here, we introduce EntoScan, a standardized, open-source hardware and software platform, provided as packaged software (https://github.com/darsa-group/EntoScan) for high-throughput imaging of arthropods, together with a new, generalized biomass estimation model that combines deep learning with a physically motivated representation of the relationship between body size and mass (https://github.com/darsa-group/BEEomass). This approach enables rapid, image-based estimation of dry biomass for large numbers of specimens (e.g., over 2,000 individuals imaged in approximately 4.5 hours), which would be impractical to measure individually using traditional

methods. We further contribute a large, openly available dataset of paired images and biomass measurements to support future work in this field (https://zenodo.org/records/20543262)

4.1 EntoScan as a standardized imaging workflow

We show how a commercially available CCD-based flatbed scanner can be adapted for imaging arthropods, and how a custom software workflow can be used to orchestrate data acquisition in a structured and reproducible way. By combining simple hardware modifications with dedicated acquisition software, EntoScan provides a practical solution for generating large, standardized image datasets of terrestrial arthropods, addressing a key bottleneck for adoption in ecological laboratories by moving towards an easy-to-use and accessible imaging platform.

Flatbed scanners have been used in a range of biological applications due to their affordability, accessibility, and ability to produce uniformly illuminated, high-resolution images. Early work by Schubert [2000] explored their use as stereoscopic imaging devices, and subsequent studies have applied scanners to diverse tasks, including fossil imaging (Schädel and Schubert [2024]), insect digitization (Ong et al. [2025], De Cesaro Júnior et al. [2022]), and environmental monitoring (Lins et al. [2020]). In addition, automated insect monitoring pipelines based on sticky trap imaging have also been developed. Keasar et al. [2024] combined scanner-acquired images of sticky cards with machine learning for large-scale data collection and analysis. These studies highlight the potential of scanners for biological imaging, particularly for capturing multiple specimens simultaneously under controlled conditions.

Despite these initiatives, there is currently no standardized workflow for generating scanner-based datasets of terrestrial arthropods. Each study employs its own setup and image acquisition protocol, resulting in variations in image quality and format. Practical challenges, such as the need to construct custom enclosures to control lighting conditions (Lins et al. [2020]), have also been reported. In addition, commercial scanner software is not designed for structured data acquisition, making it difficult to define specific scan regions or associate images with metadata.

EntoScan addresses these limitations by integrating hardware and software into a single workflow. With a simple modification of the scanner, specimens can be imaged in petri dishes and well plates while maintaining focus by repositioning them closer to the focal plane, thereby addressing the limited depth of field of flatbed scanners. The software enables selective region scanning, real-time preview, and automatic metadata association through optional barcodes.

To our knowledge, this represents the first application of such a modification for high-throughput imaging of arthropods using a flatbed scanner, making it possible to standardize image acquisition across experiments and users. In practice, the system was straightforward to adopt, and users were able to learn the workflow within a short training period. Because the platform is based on commercially available hardware, the setup can be replicated with minimal variation, further

supporting standardization.

EntoScan is provided as an open-source and documented solution, making it straightforward to deploy as an off-the-shelf workflow in different laboratories. While developed for imaging arthropods, the system is not limited to insects and can be applied to a range of biological questions involving other organisms, such as seeds or small aquatic species (e.g., fish).

4.2 Dataset generation and scalability

An important aspect of this work is the effort required to generate the training dataset. Obtaining dry biomass measurements involves drying and weighing individual specimens, which is time-consuming and limits the scale of traditional approaches. In this study, weighing a rack of 23 specimens took around 20 minutes. Even without considering the additional 24 hours typically required for drying, this process is substantially slower than the image-based approach. Using the biomass estimation model, the biomass of hundreds of insects can be estimated within minutes with reliable confidence.

Combining this biomass estimation approach with an imaging system that captures hundreds of specimens in a single acquisition makes EntoScan a powerful tool. While other vision-based approaches, including microscopy-based imaging systems, platforms such as BIODISCOVER (Ärje et al. [2020]), and large-scale specimen imaging initiatives like BIOSCAN (Gharaee et al. [2023]), typically image specimens individually, and systems such as the Entomoscope (Wührl et al. [2023]) or the method proposed by Schneider et al. [2022] can image larger areas, but they require adjustment of the imaging setup and camera distance across experiments. EntoScan instead provides a simpler and more consistent solution by maintaining a fixed imaging configuration and scanning a large area in a single pass. In addition, with improved segmentation tools such as FlatBug (Svenning et al. [2026]), it becomes feasible to scan bulk samples rather than imaging individual specimens. Although image quality may differ compared to systems that use specialized lenses or microscopy, flatbed scanners can acquire high-resolution images (e.g., up to 6400 dpi, corresponding to roughly 250 pixels per mm, meaning a 1 mm insect spans about 250 pixels), providing sufficient detail for computer vision-based analysis.

4.3 Biomass estimation as a use case

Within this framework, we explored biomass estimation as a use case. While computer vision is widely used for taxonomic classification (Baghooee and Geissmann [2026c], Grele and Richards [2026], Gharaee et al. [2024], Stevens et al. [2024] Li et al. [2021], Valan et al. [2019]) and workflows such as EntoScan can facilitate faster image acquisition for such applications, fewer studies have focused on estimating functional traits such as biomass. Existing approaches for biomass estimation typically rely on statistical relationships between body size (e.g., length or area) (Ärje et al. [2020],

Schneider et al. [2022]), or on explicit measurements of morphological features (Shirali et al. [2025]). More recently, learning-based methods have also been explored to predict biomass directly from images (Impiö et al. [2026]).

In this study, we extend these approaches by introducing the biomass factor (BF) as a size-normalized representation that allows the model to account for differences in morphology. By combining this representation with the EntoScan workflow, biomass can be estimated for large numbers of specimens in a relatively short time, with high accuracy ($R^2 = 0.95$). Because multiple individuals can be imaged simultaneously, the approach scales more efficiently than manual measurement and single-specimen imaging approaches. In essence, this approach functions as a vision-based alternative to a traditional balance, enabling rapid and scalable estimation of biomass from images.

4.4 Biological applications

The proof-of-concept analyses demonstrate the potential use of EntoScan to capture biologically meaningful variation. In *Drosophila*, the method captures expected differences in body size across species, temperature and sex. Because large numbers of individuals can be imaged and analyzed, it becomes feasible to quantify variation within populations at a much finer scale. This goes beyond comparing mean values and enables the study of within-population variation, such as changes in variance which can itself be a biologically relevant trait (Morgante et al. [2015], Ayroles et al. [2015]). In addition, the same image data also contains information that could be used for training classification models to predict species, sex, or developmental conditions.

Similarly, in the spider case study, large numbers of field-collected specimens were processed. Manually measuring dry biomass for this number of samples would be highly time-consuming. EntoScan provided a practical alternative, enabling the analysis of seasonal changes in body size and supporting studies of environmentally driven body-size variation in spiders and other arthropods (e.g., Cabon et al. [2024]). Together, these results suggest that the method can support ecological studies that require large sample sizes, including monitoring workflows where both biomass and biodiversity are of interest (Iwaszkiewicz-Eggebrecht et al. [2026]).

4.5 Limitations and future directions

While the proposed approach provides a scalable solution for estimating biomass from images, several limitations should be considered. First, the biomass factor (BF) formulation assumes a relatively consistent relationship between size and mass, such that changes in body size are predictably associated with changes in biomass. Although this approximation holds across many taxa, deviations from isometric scaling or pronounced morphological differences may introduce prediction errors. Expanding the training dataset to include a broader range of taxa and body

forms would likely improve model robustness.

Second, the approach relies on accurate segmentation of specimens from the background. While recent advances in segmentation methods, such as FlatBug (Svenning et al. [2026]), enable reliable extraction of individual specimens even from bulk images, segmentation errors may still propagate to downstream predictions, particularly in densely packed or overlapping samples.

Despite these limitations, the combination of standardized imaging, scalable acquisition, and learning-based analysis provide a strong foundation for further development. Future work could focus on improving the dataset by including a broader range of taxa and specimens collected using diverse trapping methods, extending the approach to additional biological traits, and integrating the workflow into automated monitoring systems for large-scale ecological studies.

4.6 Summary

Overall, this work shows that combining a standardized and near off-the-shelf imaging platform with a physically motivated representation of biomass provides a practical way to scale up biomass estimation. The EntoScan system enables the acquisition of high-quality, standardized images that can be used not only for established tasks such as taxonomic classification, but also for estimating functional traits such as biomass with high predictive performance. This integration of standardized imaging and quantitative analysis opens new possibilities for large-scale studies of arthropod communities.

Acknowledgments

We thank Claus Rasmussen and Tobias Andermann for providing samples collected using pan traps in Denmark and Malaise traps in Sweden, respectively. We are grateful to Jesper Smærup Bechsgaard and Giulia Soffiantini (Department of Biology, Aarhus University) for sharing the beetles and spiders for our dataset, and to Christoffer Bergvall (Evolutionary Biology Centre, Uppsala University) and Paco Cárdenas (Museum of Evolution, Uppsala University) for providing access to facilities and equipment. We also thank Toke Høye and Jarret Blair (Department of Ecoscience, Aarhus University) for their assistance with the Biodiscover dataset and Helena Russello (Center for Quantitative Genetics and Genomics, Aarhus University) for help with 3D printing components.

M. Baghooee and Q. Geissmann were supported by Novo Nordisk Foundation Start Package grant under grant number [NNF22OC0077040]. Q. Geissmann was also supported by the 2022–2023 BIODIVERSA+ joint call for research proposals, with the funding organization Innovation Fund Denmark (grant no. 2128-00003).

Author Contributions

M. Baghooee and Q. Geissmann conceived the ideas. M. Baghooee, R. Thalheim, and Q. Geissmann contributed to the implementation of the EntoScan hardware. Q. Geissmann contributed to the implementation of the EntoScan software. M. Baghooee and Q. Geissmann led the writing. F. Hasan, S. Toft, and T.N. Kristensen assisted with data collection. T.N. Kristensen designed and reared the *Drosophila* experiment. S. Toft identified and sorted the spider samples. M. Baghooee and R. Thalheim scanned the collected samples and generated the dataset. M. Baghooee and Q. Geissmann contributed to data pre-processing, training, and evaluation of the models. M. Baghooee and Q. Geissmann analysed the results. Q. Geissmann supervised the project and acquired funding. M. Baghooee wrote the original draft. All authors contributed critically to the drafts and gave final approval for publication.

Data Availability

The dataset is available on Zenodo (DOI: 10.5281/zenodo.20543262) (Baghooee and Geissmann [2026b]). The BEEomass model is also available on Zenodo (DOI: 10.5281/zenodo.20624495) (Baghooee and Geissmann [2026a]), and the code for EntoScan (github.com/darsa-group/EntoScan), and BEEomass (github.com/darsa-group/BEEomass) is available on GitHub.

References

Mark Alderweireldt and Ronny De Keer. Field and laboratory observations on the life cycle of Pachygnatha degeeri Sundevall, 1830 and Pachygnatha clercki Sundevall, 1823 (Araneae, Tetragnathidae). In *ACTA ZOOLOGICA FENNICA*, volume 190, pages 35–39, 1990. ISBN 978-951-9481-35-7. URL http://hdl.handle.net/1854/LU-01HHFA21WN8XFZASTFNEBVBZZ5. ISSN: 0001-7299.

Julien F. Ayroles, Sean M. Buchanan, Chelsea O'Leary, Kyobi Skutt-Kakaria, Jennifer K. Grenier, Andrew G. Clark, Daniel L. Hartl, and Benjamin L. De Bivort. Behavioral idiosyncrasy reveals genetic control of phenotypic variability. *Proceedings of the National Academy of Sciences*, 112 (21):6706–6711, May 2015. ISSN 0027-8424, 1091-6490. doi: 10.1073/pnas.1503830112. URL https://pnas.org/doi/full/10.1073/pnas.1503830112.

Melika Baghooee and Quentin Geissmann. BEEomass. June 2026a. doi: 10.5281/zenodo.20624495. URL https://zenodo.org/records/20624495. Publisher: Zenodo.

Melika Baghooee and Quentin Geissmann. EntoScan, June 2026b. URL https://zenodo.org/records/20543262.

Melika Baghooee and Quentin Geissmann. Insect size matters: Using image and dimensions together improves image classification. *Ecological Informatics*, 94:103664, March 2026c. ISSN 15749541. doi: 10.1016/j.ecoinf.2026.103664. URL https://linkinghub.elsevier.com/retrieve/pii/S1574954126000701.

Parzival Borlinghaus, Jörg Marvin Gülzow, and Richard Odemer. In-hive flatbed scanners for non-destructive, long-term monitoring of honey bee brood, pathogens and pests. *Smart Agricultural Technology*, 9:100655, December 2024. ISSN 27723755. doi: 10.1016/j.atech.2024.100655. URL https://linkinghub.elsevier.com/retrieve/pii/S2772375524002600.

Valentin Cabon, Hervé Quénol, Benoît Deletre, Louis Copin, Vincent Dubreuil, and Benjamin Bergerot. Body size responses to urban temperature variations are driven by life history traits in spiders. *Functional Ecology*, 38(7):1578–1589, July 2024. ISSN 1365-2435. doi: 10.1111/1365-2435.14570. URL https://besjournals.onlinelibrary.wiley.com/doi/10.1111/1365-2435.14570. Publisher: John Wiley & Sons, Ltd.

Telmo De Cesaro Júnior, Rafael Rieder, Jéssica Regina Di Domênico, and Douglas Lau. InsectCV: A system for insect detection in the lab from trap images. *Ecological Informatics*, 67:101516, March 2022. ISSN 15749541. doi: 10.1016/j.ecoinf.2021.101516. URL https://linkinghub.elsevier.com/retrieve/pii/S1574954121003071.

Michael L. Ferro and Morgan Summerlin. Developing a standardized p of entomological collection methods for use in databases. *ZooKeys*, 861:145–156, July 2019. ISSN 1313-2970, 1313-2989. doi: 10.3897/zookeys.861.32347. URL https://zookeys.pensoft.net/article/32347/.

Quentin Geissmann, Paul K. Abram, Di Wu, Cara H. Haney, and Juli Carrillo. Sticky Pi is a high-frequency smart trap that enables the study of insect circadian activity under natural conditions. *PLOS Biology*, 20(7):e3001689, July 2022. ISSN 1545-7885. doi: 10.1371/journal.pbio.3001689. URL https://dx.plos.org/10.1371/journal.pbio.3001689.

Zahra Gharaee, ZeMing Gong, Nicholas Pellegrino, Iuliia Zarubiieva, Joakim Bruslund Haurum, Scott C. Lowe, Jaclyn T. A. McKeown, Chris C. Y. Ho, Joschka McLeod, Yi-Yun C. Wei, Jireh Agda, Sujeevan Ratnasingham, Dirk Steinke, Angel X. Chang, Graham W. Taylor, and Paul Fieguth. A Step Towards Worldwide Biodiversity Assessment: The BIOSCAN-1M Insect Dataset, July 2023. URL http://arxiv.org/abs/2307.10455. arXiv:2307.10455 [cs].

Zahra Gharaee, Scott C. Lowe, ZeMing Gong, Pablo Millan Arias, Nicholas Pellegrino, Austin T. Wang, Joakim Bruslund Haurum, Iuliia Zarubiieva, Lila Kari, Dirk Steinke, Graham W. Taylor, Paul Fieguth, and Angel X. Chang. BIOSCAN-5M: A Multimodal Dataset for Insect Biodiversity, November 2024. URL http://arxiv.org/abs/2406.12723. arXiv:2406.12723 [cs].

Ari Grele and Lora A. Richards. BugNet: a rapid and scalable pipeline for automated insect monitoring using hierarchical data. *Frontiers in Ecology and Evolution*, 14:1750931, February 2026. ISSN 2296-701X. doi: 10.3389/fevo.2026.1750931. URL https://www.frontiersin.org/articles/10.3389/fevo.2026.1750931/full.

Caspar A. Hallmann, Martin Sorg, Eelke Jongejans, Henk Siepel, Nick Hofland, Heinz Schwan, Werner Stenmans, Andreas Müller, Hubert Sumser, Thomas Hörren, Dave Goulson, and Hans De Kroon. More than 75 percent decline over 27 years in total flying insect biomass in protected areas. *PLOS ONE*, 12(10):e0185809, October 2017. ISSN 1932-6203. doi: 10.1371/journal.pone.0185809. URL https://dx.plos.org/10.1371/journal.pone.0185809.

Mikko Impiö, Philipp M. Rehsen, Jarrett Blair, Cecilie Mielec, Arne J. Beermann, Florian Leese, Toke T. Høye, and Jenni Raitoharju. Computer vision-based estimation of invertebrate biomass, March 2026. URL http://arxiv.org/abs/2603.06362. arXiv:2603.06362 [cs.CV].

Ela Iwaszkiewicz-Eggebrecht, Emma Granqvist, Karol H. Nowak, Catalina Valdivia, Mateusz Buczek, Amrita Srivathsan, Emily Hartop, Andreia Miraldo, Tomas Roslin, Ayco J. M. Tack, Piotr Łukasik, Rudolf Meier, and Fredrik Ronquist. Accuracy of occurrence and abundance estimates from insect metabarcoding. *bioRxiv*, page 2026.02.20.707016, February 2026. ISSN 2692-8205. doi: 10.64898/2026.02.20.707016. URL https://pmc.ncbi.nlm.nih.gov/articles/PMC12934785/.

D. Karan, J.P. Morin, B. Moreteau, and J.R. David. Body size and developmental temperature in drosophila melanogaster: analysis of body weight reaction norm. *Journal of Thermal Biology*, 23(5):301–309, October 1998. ISSN 03064565. doi: 10.1016/S0306-4565(98)00021-7. URL https://linkinghub.elsevier.com/retrieve/pii/S0306456598000217.

Dave Karlsson, Emily Hartop, Mattias Forshage, Mathias Jaschhof, and Fredrik Ronquist. The Swedish Malaise Trap Project: A 15 Year Retrospective on a Countrywide Insect Inventory. *Biodiversity Data Journal*, 8:e47255, January 2020. ISSN 1314-2828, 1314-2836. doi: 10.3897/BDJ.8.e47255. URL https://bdj.pensoft.net/article/47255/.

Tamar Keasar, Michael Yair, Daphna Gottlieb, Liraz Cabra-Leykin, and Chen Keasar. STARdbi: A pipeline and database for insect monitoring based on automated image analysis. *Ecological Informatics*, 80:102521, May 2024. ISSN 15749541. doi: 10.1016/j.ecoinf.2024.102521. URL https://linkinghub.elsevier.com/retrieve/pii/S1574954124000633.

Liam K. Kendall, Romina Rader, Vesna Gagic, Daniel P. Cariveau, Matthias Albrecht, Katherine C. R. Baldock, Breno M. Freitas, Mark Hall, Andrea Holzschuh, Francisco P. Molina, Joanne M. Morten, Janaely S. Pereira, Zachary M. Portman, Stuart P. M. Roberts, Juanita Rodriguez, Laura Russo, Louis Sutter, Nicolas J. Vereecken, and Ignasi Bartomeus. Pollinator size and its consequences: Robust estimates of body size in pollinating insects. *Ecology and Evolution*,

9(4):1702–1714, February 2019. ISSN 2045-7758, 2045-7758. doi: 10.1002/ece3.4835. URL https://onlinelibrary.wiley.com/doi/10.1002/ece3.4835.

Nataliya Kovtonyuk, Irina Han, and Evgeniya Gatilova. Digital Herbarium Collections of the Central Siberian Botanical Garden SB RAS, Novosibirsk, Russia. In Igor Bychkov and Victor Voronin, editors, *Information Technologies in the Research of Biodiversity*, pages 22–27, Cham, 2019. Springer International Publishing. ISBN 978-3-030-11720-7. doi: 10.1007/978-3-030-11720-7_4.

Sara Kühsel, Adrian Brückner, Sebastian Schmelzle, Michael Heethoff, and Nico Blüthgen. Surface area–volume ratios in insects. *Insect Science*, 24(5):829–841, October 2017. ISSN 1672-9609, 1744-7917. doi: 10.1111/1744-7917.12362. URL https://onlinelibrary.wiley.com/doi/10.1111/1744-7917.12362.

Wenyong Li, Tengfei Zheng, Zhankui Yang, Ming Li, Chuanheng Sun, and Xinting Yang. Classification and detection of insects from field images using deep learning for smart pest management: A systematic review. *Ecological Informatics*, 66:101460, December 2021. ISSN 15749541. doi: 10.1016/j.ecoinf.2021.101460. URL https://linkinghub.elsevier.com/retrieve/pii/S157495412100251X.

Elison Alfeu Lins, João Pedro Mazuco Rodriguez, Sandy Ismael Scoloski, Juliana Pivato, Marília Balotin Lima, José Maurício Cunha Fernandes, Paulo Roberto Valle Da Silva Pereira, Douglas Lau, and Rafael Rieder. A method for counting and classifying aphids using computer vision. *Computers and Electronics in Agriculture*, 169:105200, February 2020. ISSN 01681699. doi: 10.1016/j.compag.2019.105200. URL https://linkinghub.elsevier.com/retrieve/pii/S0168169919306039.

Bradford C. Lister and Andres Garcia. Climate-driven declines in arthropod abundance restructure a rainforest food web. *Proceedings of the National Academy of Sciences*, 115(44), October 2018. ISSN 0027-8424, 1091-6490. doi: 10.1073/pnas.1722477115. URL https://pnas.org/doi/full/10.1073/pnas.1722477115.

Heidi J. MacLean, Jesper G. Sørensen, Torsten N. Kristensen, Volker Loeschcke, Kristian Beedholm, Vanessa Kellermann, and Johannes Overgaard. Evolution and plasticity of thermal performance: an analysis of variation in thermal tolerance and fitness in 22 Drosophila species. *Philosophical Transactions of the Royal Society B: Biological Sciences*, 374(1778):20180548, August 2019. ISSN 0962-8436. doi: 10.1098/rstb.2018.0548. URL https://pmc.ncbi.nlm.nih.gov/articles/PMC6606468/.

Stylianos Mavrianos, Sven Teurlincx, Steven Aj Declerck, and Kathrin A Otte. HiReS: A Method for Automated Morphometric Trait Extraction from High-Resolution Plankton Images, April 2026. URL http://biorxiv.org/lookup/doi/10.64898/2026.04.11.717915.

Patina K. Mendez, Sangyeon Lee, and Chris E. Venter. Imaging natural history museum collections from the bottom up: 3D print technology facilitates imaging of fluid-stored arthropods with flatbed scanners. *ZooKeys*, 795:49–65, November 2018. ISSN 1313-2970, 1313-2989. doi: 10.3897/zookeys.795.28416. URL https://zookeys.pensoft.net/articles.php?id=28416.

Graham A. Montgomery, Michael W. Belitz, Rob P. Guralnick, and Morgan W. Tingley. Standards and Best Practices for Monitoring and Benchmarking Insects. *Frontiers in Ecology and Evolution*, 8:579193, January 2021. ISSN 2296-701X. doi: 10.3389/fevo.2020.579193. URL https://www.frontiersin.org/articles/10.3389/fevo.2020.579193/full.

Fabio Morgante, Peter Sørensen, Daniel A. Sorensen, Christian Maltecca, and Trudy F. C. Mackay. Genetic Architecture of Micro-Environmental Plasticity in Drosophila melanogaster. *Scientific Reports*, 5(1):9785, May 2015. ISSN 2045-2322. doi: 10.1038/srep09785. URL https://www.nature.com/articles/srep09785.

Song-Quan Ong, Nathan Pinoy, Min Hui Lim, Kim Bjerge, Francisco Javier Peris-Felipo, Rob Lind, Jordan P. Cuff, Samantha M. Cook, and Toke Thomas Høye. ScannerVision: Scanner-based image acquisition of medically important arthropods for the development of computer vision and deep learning models. *Current Research in Parasitology & Vector-Borne Diseases*, 7:100268, 2025. ISSN 2667114X. doi: 10.1016/j.crpvbd.2025.100268. URL https://linkinghub.elsevier.com/retrieve/pii/S2667114X25000287.

Adam Paszke, Sam Gross, Francisco Massa, Adam Lerer, James Bradbury, Gregory Chanan, Trevor Killeen, Zeming Lin, Natalia Gimelshein, Luca Antiga, Alban Desmaison, Andreas Köpf, Edward Yang, Zach DeVito, Martin Raison, Alykhan Tejani, Sasank Chilamkurthy, Benoit Steiner, Lu Fang, Junjie Bai, and Soumith Chintala. PyTorch: An Imperative Style, High-Performance Deep Learning Library, December 2019. URL http://arxiv.org/abs/1912.01703. arXiv:1912.01703 [cs].

R Core Team R Core Team. R: A Language and Environment for Statistical Computing. Technical Report Version 4.5.2, R Foundation for Statistical Computing, Vienna, Austria, 2025. URL https://www.r-project.org/.

Stefan Schneider, Graham W. Taylor, Stefan C. Kremer, Patrick Burgess, Jillian McGroarty, Kyomi Mitsui, Alex Zhuang, Jeremy R. deWaard, and John M. Fryxell. Bulk arthropod abundance, biomass and diversity estimation using deep learning for computer vision. *Methods in Ecology and Evolution*, 13(2):346–357, February 2022. ISSN 2041-210X, 2041-210X. doi: 10.1111/2041-210X.13769. URL https://besjournals.onlinelibrary.wiley.com/doi/10.1111/2041-210X.13769.

R. Schubert. Using a flatbed scanner as a stereoscopic near-field camera. *IEEE Computer Graphics*

and Applications, 20(2):38–45, March 2000. ISSN 0272-1716, 1558-1756. doi: 10.1109/38.824535. URL https://ieeexplore.ieee.org/document/824535/.

Mario Schädel and Richard Schubert. Flatbed scanners as versatile tools for studying surface details of compression fossils. *Palaeontologia Electronica*, 2024. ISSN 19353952, 10948074. doi: 10.26879/1353. URL https://palaeo-electronica.org/content/2024/5216-scanning-fossil-surfaces.

Hossein Shirali, Aleida Ascenzi, Lorenz Wührl, Nils Beyer, Noemi Di Lorenzo, Emanuele Vaccarella, Nathalie Klug, Rudolf Meier, Pierfilippo Cerretti, and Christian Pylatiuk. InsectMorphoAI: A Deep Learning-Based Software for Automated Estimation of Insect Length, Volume, and Biomass, May 2025. URL http://biorxiv.org/lookup/doi/10.1101/2025.05.22.655251.

Maximilian Sittinger, Johannes Uhler, Maximilian Pink, and Annette Herz. Insect detect: An open-source DIY camera trap for automated insect monitoring. *PLOS ONE*, 19(4):e0295474, April 2024. ISSN 1932-6203. doi: 10.1371/journal.pone.0295474. URL https://dx.plos.org/10.1371/journal.pone.0295474.

Samuel Stevens, Jiaman Wu, Matthew J. Thompson, Elizabeth G. Campolongo, Chan Hee Song, David Edward Carlyn, Li Dong, Wasila M. Dahdul, Charles Stewart, Tanya Berger-Wolf, Wei-Lun Chao, and Yu Su. BioCLIP: A Vision Foundation Model for the Tree of Life, May 2024. URL http://arxiv.org/abs/2311.18803. arXiv:2311.18803 [cs.CV].

Asger Svenning, Guillaume Mougeot, Jamie Alison, Daphne Chevalier, Nisa Chavez Molina, Song-Quan Ong, Kim Bjerge, Juli Carrillo, Toke Thomas Høye, and Quentin Geissmann. A general method for detection and segmentation of terrestrial arthropods in images. *Methods in Ecology and Evolution*, 17(3):727–739, March 2026. ISSN 2041-210X, 2041-210X. doi: 10.1111/2041-210x.70249. URL https://besjournals.onlinelibrary.wiley.com/doi/10.1111/2041-210x.70249.

Mingxing Tan and Quoc V Le. EfficientNet: Rethinking Model Scaling for Convolutional Neural Networks. *Proceedings of the 36th International Conference on Machine Learning*, 97:6105–6114, 2019.

Johannes Uhler, Sarah Redlich, Jie Zhang, Torsten Hothorn, Cynthia Tobisch, Jörg Ewald, Simon Thorn, Sebastian Seibold, Oliver Mitesser, Jérôme Morinière, Vedran Bozicevic, Caryl S. Benjamin, Jana Englmeier, Ute Fricke, Cristina Ganuza, Maria Haensel, Rebekka Riebl, Sandra Rojas-Botero, Thomas Rummler, Lars Uphus, Stefan Schmidt, Ingolf Steffan-Dewenter, and Jörg Müller. Relationship of insect biomass and richness with land use along a climate gradient. *Nature Communications*, 12(1):5946, October 2021. ISSN 2041-1723. doi: 10.1038/s41467-021-26181-3. URL https://www.nature.com/articles/s41467-021-26181-3.

Miroslav Valan, Karoly Makonyi, Atsuto Maki, Dominik Vondráček, and Fredrik Ronquist. Automated Taxonomic Identification of Insects with Expert-Level Accuracy Using Effective Feature Transfer from Convolutional Networks. *Systematic Biology*, 68(6):876–895, November 2019. ISSN 1063-5157, 1076-836X. doi: 10.1093/sysbio/syz014. URL https://academic.oup.com/sysbio/article/68/6/876/5368535.

Nicolas J. Vereecken, Timothy Weekers, Nicolas Leclercq, Stéphane De Greef, Hélène Hainaut, Jean-Marc Molenberg, Youri Martin, Xavier Janssens, Grégoire Noël, Alain Pauly, Stuart P.M. Roberts, and Leon Marshall. Insect biomass is not a consistent proxy for biodiversity metrics in wild bees. *Ecological Indicators*, 121:107132, February 2021. ISSN 1470160X. doi: 10.1016/j.ecolind.2020.107132. URL https://linkinghub.elsevier.com/retrieve/pii/S1470160X20310712.

Hadley Wickham. *ggplot2: Elegant Graphics for Data Analysis*. Use R! Springer International Publishing : Imprint: Springer, Cham, 2nd ed. 2016 edition, 2016. ISBN 978-3-319-24277-4. doi: 10.1007/978-3-319-24277-4.

Lorenz Wührl, Luca Rettenberger, Rudolf Meier, Emily Hartop, Julien Graf, and Christian Pylatiuk. Entomoscope: An Open-Source Photomicroscope for Biodiversity Discovery, September 2023. URL https://www.techrxiv.org/doi/full/10.36227/techrxiv.24101214.v1.

Louie H Yang and Claudio Gratton. Insects as drivers of ecosystem processes. *Current Opinion in Insect Science*, 2:26–32, August 2014. ISSN 22145745. doi: 10.1016/j.cois.2014.06.004. URL https://linkinghub.elsevier.com/retrieve/pii/S2214574514000339.

Johanna Ärje, Claus Melvad, Mads Rosenhøj Jeppesen, Sigurd Agerskov Madsen, Jenni Raitoharju, Maria Strandgård Rasmussen, Alexandros Iosifidis, Ville Tirronen, Moncef Gabbouj, Kristian Meissner, and Toke Thomas Høye. Automatic image-based identification and biomass estimation of invertebrates. *Methods in Ecology and Evolution*, 11(8):922–931, August 2020. ISSN 2041-210X, 2041-210X. doi: 10.1111/2041-210X.13428. URL https://besjournals.onlinelibrary.wiley.com/doi/10.1111/2041-210X.13428.

Supplementary material

S1- Video. Demonstration of the EntoScan imaging setup and acquisition workflow. Available at: https://doi.org/10.6084/m9.figshare.32406576.

Table 1: Number of *Drosophila* individuals per species and temperature treatment.

Species	**19°C**	**28°C**	**Total**
D. equinoxialis	121	115	236
D. lutescens	271	281	552
D. melanogaster	356	192	548
D. simulans	219	251	470
D. virilis	128	136	262
Total	1095	975	2070